



Microstructure characterization and electrical transport of nanocrystalline $\text{Zn}_{0.90}\text{Mn}_{0.10}\text{O}$ semiconductors synthesized by mechanical alloying

S. Choudhury^a, S. Sain^b, M.K. Mandal^a, S.K. Pradhan^b, A.K. Meikap^{a,*}

^a Department of Physics, National Institute of Technology, Durgapur 713209, West Bengal, India

^b Department of Physics, The University of Burdwan, Golapbag, Burdwan 713104, West Bengal, India

ARTICLE INFO

Article history:

Received 24 April 2015

Received in revised form 28 September 2015

Accepted 12 January 2016

Available online 15 January 2016

Keywords:

- A. Nanostructures
- B. Microstructure
- C. X-ray diffractions
- D. Electrical properties
- D. Dielectric properties

ABSTRACT

We report a comprehensive study of dc and ac conductivity, dielectric relaxation and capacitance–voltage characteristics of Mn doped ZnO nanocrystalline semiconductors prepared by mechanical alloying. Samples are characterized by HRTEM and XRD. Direct current conductivity increases with the increase in temperature and the thermal behavior of electrical dc conductivity for the investigated samples can be described by adiabatic polaronic hopping model. The frequency dependent conductivity obeys a power law $\sigma'(f) \propto f^s T^n$. The temperature exponent n strongly depends on frequency. Analysis of the temperature dependence of frequency exponent s suggests a transformation from large polaron to small polaron conduction model with increase in temperature. Considering electric modulus the dielectric properties of the samples have been explained. Capacitance–voltage characteristic suggests the formation of Schottky diode between metallic electrode and semiconductor junction and diode parameter shows anomalous behavior with increasing milling time.

© 2016 Elsevier Ltd. All rights reserved.

1. Introduction

Zinc oxide is a wide band gap semiconductor which plays a very significant role in many industrial applications [1–6]. However, ZnO based solid solutions with transition metal oxides have substantial interest due to their combined semiconducting and magnetic properties. Such materials are called dilute magnetic semiconductors (DMS), which have unique properties like large exciton binding energy, high energy band gap and large optical gain. This enhanced behavior of the materials would be suitable for optoelectronic and magneto-optical devices [7]. During the last few decades, the II–VI and III–V group elements are studied mostly due to their spintronic application which inspired the researchers to synthesize DMS materials by using II–VI and III–V semiconductors [8–13]. In such materials the cations of semiconductors materials are replaced by transition metals ions. As a result the d electron of magnetic ions interact with the carriers of the band of semiconductor and produces spin–spin exchange interaction which leads various interesting properties like large Zeeman splitting of the states of energy band and enhanced Faraday effect

[7]. Different growth techniques like sol–gel method, molecular beam epitaxy, rf magnetron sputtering, pulse laser deposition technique and ultrasonic spray pyrolysis technique have been used for the preparation of Mn doped ZnO samples [14–17]. However, the synthesis by mechanical alloying method is not used very much. Sain et al. [18] has reported first time about the preparation of Mn doped ZnO nanocrystal by mechanical alloying. They have reported microstructural, magnetic and optical characterization of nanocrystalline $\text{Zn}_{1-x}\text{Mn}_x\text{O}$ at room temperature. Chen et al. [19] studied magneto-optical properties of Mn doped ZnO films prepared by ultrasonic spray pyrolysis. Milivojevic et al. [20] and Jayakumar et al. [21] reported the room temperature ferromagnetic behavior of Mn doped ZnO prepared by solid state reaction. Although some studies have been reported on magneto-optical and magneto-electrical properties of Mn-doped ZnO nanocrystalline DMS [7,19], the electrical and dielectric properties have been reported very few [22]. Yalishev et al. [23] have reported the influence of Mn-oxide nanoclusters on the I–V and C–V characterizes of ZnO:Mn films. Dhananjay et al. [22] have reported the dc and ac electrical transport properties of Mn-doped ZnO thin films grown by pulsed laser ablation. Generally the conduction mechanism in ionic conductors can be explained by using

* Corresponding author. Fax: +91 343 2547375.

E-mail address: meikapnritd@yahoo.com (A.K. Meikap).

impedance spectroscopy basically by analysis the power law of frequency dependent conductivity.

The aims of the present study are (1) to prepare the nanocrystalline Mn doped ZnO samples at room temperature by high energy ball milling process. (2) To characterize the prepared samples by analyzing the X-ray diffraction profiles. (3) The systematic study of electric transport behavior like dc conductivity, ac conductivity, dielectric properties and C–V characteristics of the investigated samples in the temperature range 298–523 K and the frequency range 20 Hz–1 MHz.

2. Experimental

Stoichiometric nanocrystalline $\text{Zn}_{0.9}\text{Mn}_{0.1}\text{O}$ is synthesized by mechanical alloying (MA) the metal oxide precursors, ZnO (E. Merck, 99% pure) and MnO (Alfa Aesar, 99.5% pure) powders. Accurately weighed (maintaining stoichiometry) ZnO and MnO powders are taken in an agate mortar for hand grinding the powder precursors for 30 min to obtain a homogeneous mixture. The mixture is then put in a chrome steel bowl of volume 80 ml containing 30 chrome steel balls with 10 mm diameter. The bowl is then mounted on the rotation disk of a high energy planetary ball mill (Fritsch, GmbH, Germany) for MA at room temperature. The milling has been carried out for different durations for the formation of MnO doped ZnO compound and the progress of milling is monitored at different time interval by analyzing the XRD pattern of a small part of the milled sample. XRD patterns of the unmilled powder mixture and all ball milled samples are recorded using Ni filtered $\text{CuK}\alpha$ radiation with 40 kV/20 mA rating from an automated and highly stabilized Philips X-ray generator (PW 1830). Step-scan data (of step size $0.05^\circ 2\theta$ and counting time 5–10 s depending on the peak intensity) are recorded for the entire range from 25° to $80^\circ 2\theta$.

Microstructure of the prepared samples is characterized by a high resolution transmission electron microscope (HRTEM) (JEOL JEM 2010, Japan) attached to GATAN CCD camera operated at 200 kV. To prepare the sample for transmission electron microscopy, very small amount of the prepared sample is dispersed into ethanol and sonicated vigorously for a long duration to obtain a homogeneous colloidal solution. A small droplet of it is then sprinkled on a carbon coated Cu grid (300 meshes). This grid is then dried completely and subsequently used for transmission microscopy. The thermal properties of the samples has been studied by using DTA-TGA, STA 600, PerkinElmer, where the samples are heated at a rate of $10^\circ\text{C}/\text{min}$ in argon atmosphere. To measure the dc and ac conductivity and dielectric response, samples are prepared as 1 cm diameter pellets by pressing the powder under a hydraulic pressure at 500 MPa. The electrical dc conductivity of the samples was measured by a standard four probe method using an $8^{1/2}$ -digit Agilent 3458A Multimeter. The fine copper wire was connected with the samples by highly conducting graphite adhesive (Electrodag 5513, Acheson, Williston, VT) for electrical measurement. The ac measurement was carried out with an E4980A Agilent Impedance analyzer up to the frequency 2 MHz at different temperatures. A high temperature cryostat was used to study the high temperature property of the samples in the range 298–523 K. The capacitance (C_p) and the dissipation factor (D) are measured at various frequencies and temperatures. The real part of ac conductivity and real and imaginary part of dielectric permittivity have been calculated using the relations $\sigma'(f) = 2\pi f \epsilon_0 \epsilon''(f)$, $\epsilon'(f) = C_p d / \epsilon_0 A$ and $\epsilon''(f) = \epsilon'(f) D$ respectively, where $\epsilon_0 = 8.854 \times 10^{-12} \text{ F/m}$, A and d are the area and thickness of the sample respectively. C_p is the capacitance; f is the frequency in Hz. The detailed experimental technique is reported in previous publication [24,25].

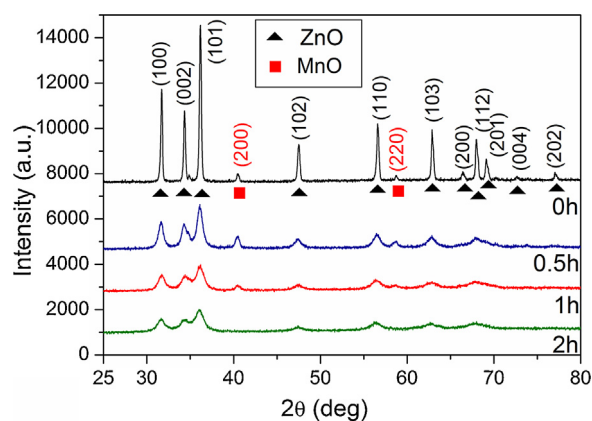


Fig. 1. Indexed XRD patterns of unmilled (0 h) and ball milled ZnO and MnO powder mixtures for different durations.

3. Results and discussion

XRD patterns of unmilled (0 h) and ball milled ZnO and MnO powder mixtures are shown in Fig. 1. All the reflections of the patterns are identified properly with hexagonal ZnO (ICSD database no. 65121, Sp. Gr. $P6_3mc$, lattice parameters: $a = 3.25682 \text{ \AA}$ and $c = 5.21251 \text{ \AA}$) and cubic MnO (ICSD database no. 643195, Sp. Gr. $Fm\bar{3}m$, lattice parameter $a = 4.4440 \text{ \AA}$) phases only. There is no Bragg reflection other than the precursors for all the patterns which suggests that there is no impurity coming either from the milling media or from the atmosphere. All the reflections of 2 h milled sample are solely composed of ZnO phase which excludes the presence of any secondary phase segregation appearing due to the multiple valences of Mn (MnO , MnO_2 , Mn_2O_3 , Mn_3O_4 , ZnMn_2O_4 , etc.) confirming the formation of pristine ZnO. Karamat et al. [26] and some other researchers [27] noticed such type of secondary phases during the formation of the material. All reflections of unmilled sample are quite sharp, well resolved and at higher scattering angle split clearly into $\text{Cu K}\alpha_{1-2}$ doublets which suggest that the particle size of the ingredient powders are quite large and particles contain minimum lattice strain. With increasing milling time, full width at half maximum (FWHM) value of each peak increases which suggests that the particle size decreases with the milling time. In the XRD pattern of the unmilled sample two prominent reflections of MnO phase are observed at $\sim 40.5^\circ 2\theta$ and $58.7^\circ 2\theta$. After 2 h of milling reflections from these peaks are completely absent which confirms the full formation of (Zn,Mn)O solid solution due to the substitution of Zn^{2+} by Mn^{2+} ions. It is interesting to notice that (200) and (220) reflections of MnO in unmilled sample become more pronounced in 0.5 h milled sample and then gradually vanished after 2 h of milling which can be explained by the fact that a portion of the ZnO diffuses into MnO lattice enhancing the peak intensity of MnO at the primary stage of milling (0.5 h). After further milling the diffused ZnO comes out from MnO lattice and reflection from MnO phase starts diminishing. Detailed structural and micro/nano structure parameters of the prepared samples have been analyzed by the method of Rietveld analysis [28,29] and reported in our earlier work [18]. Different structural and micro/nano structure parameters obtained from the Rietveld analysis are tabulated in Table 1.

Selected area electron diffraction (SAED) pattern of 2 h milled $\text{Zn}_{0.90}\text{Mn}_{0.10}\text{O}$ is shown in Fig. 2. All diffraction rings are indexed accordingly. Here, it is noticed that the diffraction ring produced by (002) plane is apparently missing. This is due to the fact that the intensity of (002) reflection is smaller than that of its adjacent (100) and (101) planes (Fig. 1). Hence, the diffraction ring produced by (002) remains unnoticed in between the two most

Download English Version:

<https://daneshyari.com/en/article/1487439>

Download Persian Version:

<https://daneshyari.com/article/1487439>

[Daneshyari.com](https://daneshyari.com)